

Structural Characterization of Electron Beam Evaporated Indium Antimonide Thin Films

Rahul*, S. R. Vishwakarma, Ravishankar Nath Tripathi and Aneet Kumar Verma
*Advance Thin Film Laboratory, Department of Physics & Electronics,
 Dr. R. M. L. Avadh University, Faizabad, U.P., India*

Indium antimonide thin films of different thickness (300-400nm) deposited by electron beam evaporation technique on suitable ultrasonically cleaned glass substrates at different substrate temperature (303-373K) are of polycrystalline nature having zinc blende structure. For $T_s \geq 303$, all deposited films have orientation along (111) and (220) planes. Some other orientations like (012), (101), (202), and (112) are also observed in the films depending upon the film thickness and substrate temperature of deposition. The values of grain size, dislocation density, strain, and lattice constant 'a' for (111) of the deposited films are calculated, and their variations with substrate temperature and films thickness are studied. The surface morphological study of thin films reveals the crystalline nature, which was in good agreement with the XRD crystallinity analysis.

1. Introduction

Conventionally, due to their structure III-V semiconductors play a major role in scientific research and its applications. The non-stoichiometric (anions and cations vacancy) in thin films of semiconducting materials is responsible for conductivity, which is created during the deposition of thin films. Initially, we have grown non-stoichiometric starting materials for fabrication of thin films. Among the III-V binary semiconductors, indium antimonide is an important semiconductor for the preparation of various devices, which has melting point 525 °C. It is a narrow band gap semiconductor with an energy band gap of 0.17 eV at 300 K, 0.23 eV at 80 K. In n-type indium antimonide semiconductor (anion vacancy) the electron has high electron mobility (80,000 cm²/V.s) due to their smaller effective mass. Similarly in p-type InSb semiconductor (cation vacancy), the hole has mobility 1250 cm²/V.s and thus it is the best material available for magnetic-field sensing devices such as Hall sensor and magnetoresistors [1], speed-sensitive sensors [2] and magnetic sensors [3]. Many reports are available on the growth of InSb thin films using different techniques such as Molecular beam epitaxy (MBE) [4], metal organic chemical vapor deposition and vacuum evaporation [5]. Of all these methods used to prepare InSb thin films, the electron beam evaporation technique is a very simple and inexpensive and can be used for large area deposition.

The aim of this work is to increase the efficiency and reduce the delay time of devices. Thin films of InSb prepared by electron beam evaporation techniques have controlled the non-stoichiometric films. The indium antimonide infrared detectors are sensitive between 3-5 μm wavelengths [6]. This material can also be used as a bio-sensor to detect the bacteria. In this paper, we report some correlative results of different structural parameters with substrate temperature and film thickness.

2. Experimental

Thin films of InSb of different thickness (t), (300-400nm), were deposited at different substrate temperature (T_s), (303-373K), on chemically and ultrasonically cleaned glass substrate with the help of a Hind Hivac Vacuum Coating unit at a vacuum value better than 10⁻⁵Torr. The source distance from glass substrate was maintained at 125mm for all cases. Non-stoichiometric materials (InSb) having composition In_{0.66}Sb_{0.34} was used as the source material. The source temperature and thus the deposition rate (0.3- 18nm/s) were adjusted by changing the electrical current of electron beam gun. In this study, the deposition rate was evaluated by a suitably designed thickness monitor using quartz crystal sensor (6 MHz) set up near the substrate. During the deposition, the film thickness was always measured by the thickness monitor and the film of different thickness was prepared for characterization. The X-Ray Diffractogram of thin films was obtained by Philips Analytical X-ray Diffractometer (PW-3710) operated at 40 kV/20

*rhl.jaunpur@gmail.com

mA using CuK_{α1} radiation with a wavelength of 1.5404 Å in angle region from 20° to 70°.

3. Structural Parameters

3.1 Determination of grain size

The grain size (D_{hkl}) for the electron beam evaporated InSb thin films are calculated with the help of Debye Scherrer's formula using the full-width at half-maximum (FWHM) β of the peaks [7].

$$D = \frac{0.94\lambda}{\beta \cos \theta} \quad (1)$$

Where β is the width of the peak at the half of maximum peaks intensity, where λ is the wavelength of X-ray used and θ is the diffraction angle.

3.2 Dislocation density

Dislocations are imperfections in a crystal and associated with the mis-registry of the lattice in one part of the crystal with respect to another part. Unlike vacancies and interstitial atoms, dislocations are not equilibrium imperfections. In fact, the growth mechanism involving dislocation is a matter of importance. The dislocation densities of thin films are given by the Williamson and Smallman's relation [8].

$$\delta = \frac{n}{D^2} \quad (2)$$

Where n is factor, which equals unity, giving minimum dislocation density and D is the grain size.

3.3 Strain

The strain is a manifestation of dislocation network in thin films. The strain in thin films can be calculated from the relation [9]

$$\beta = \frac{\lambda}{D \cos \theta} - \varepsilon \tan \theta \quad (3)$$

Where θ is Bragg's angle, β is the width of the peak at half of the maximum peaks intensity, and ε is the strain.

3.4 Determination of lattice constant

The lattice parameter, a, for cubic phase structure (h k l) is determined by the relation

$$d_{hkl} = \frac{a}{(h^2 + k^2 + l^2)^{1/2}} \quad (4)$$

Where $N=h^2+k^2+l^2$ is a number. Observing the distribution of N values, the type of the cubic lattice can be determined [10].

From the Bragg's law,

$$\lambda = \frac{2a \sin \theta}{(h^2 + k^2 + l^2)^{1/2}}$$

Or

$$\sin^2 \theta = \left(\frac{\lambda^2}{4a^2} \right) (h^2 + k^2 + l^2) = \frac{\lambda^2 N}{4a^2} \quad (5)$$

For hexagonal crystals, the lattice constants, a, and, c, are evaluated from the following relations

$$\frac{1}{d^2} = \left[\left(\frac{4}{3} \right) \left\{ \frac{h^2 + k^2 + l^2}{a^2} \right\} \right] + \left(\frac{l^2}{c^2} \right)$$

From Bragg's law

$$\sin^2 \theta = \left(\frac{\lambda^2}{3} \right) \left[\left\{ \frac{h^2 + k^2 + hk}{a^2} \right\}^2 \right] + \frac{\lambda^2 l^2}{4c^2}$$

According to Vegards law, the lattice parameters of hexagonal unit cell are related to cubic lattice parameters of the same material as

$$\begin{aligned} a_{hex} &= \left(\frac{1}{2} \right)^{1/2} a_{cubic} \\ c_{hex} &= \left(\frac{4}{3} \right)^{1/2} a_{cubic} \end{aligned} \quad (6)$$

Hence for an 'ideal' Wurtzite lattice, the relation between the two lattice parameters is

$$c_{hex} = (1.633)a_{hex}$$

Which can be used for the calculation of lattice parameters of InSb thin films?

There are several possible sources of error, such as the divergence of X-ray beams, refraction and absorption of X-rays by the specimen etc., in the measurement of θ and d values. Therefore, the accuracy in the determination of lattice constant is dependent upon the accuracy of their measurements.

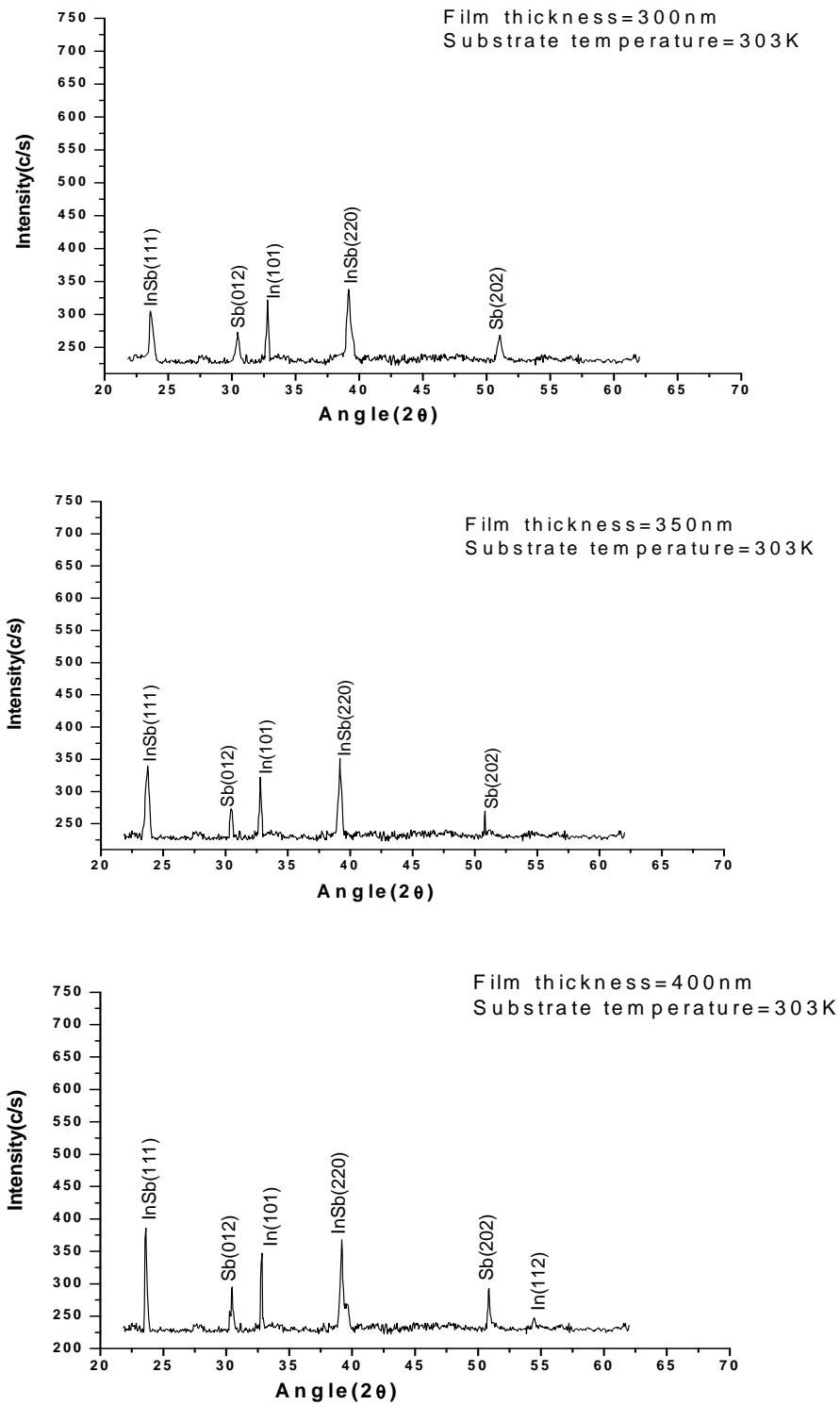


Fig.1: XRD patterns of InSb thin films of different thickness and deposited at same $T_s=303$ K

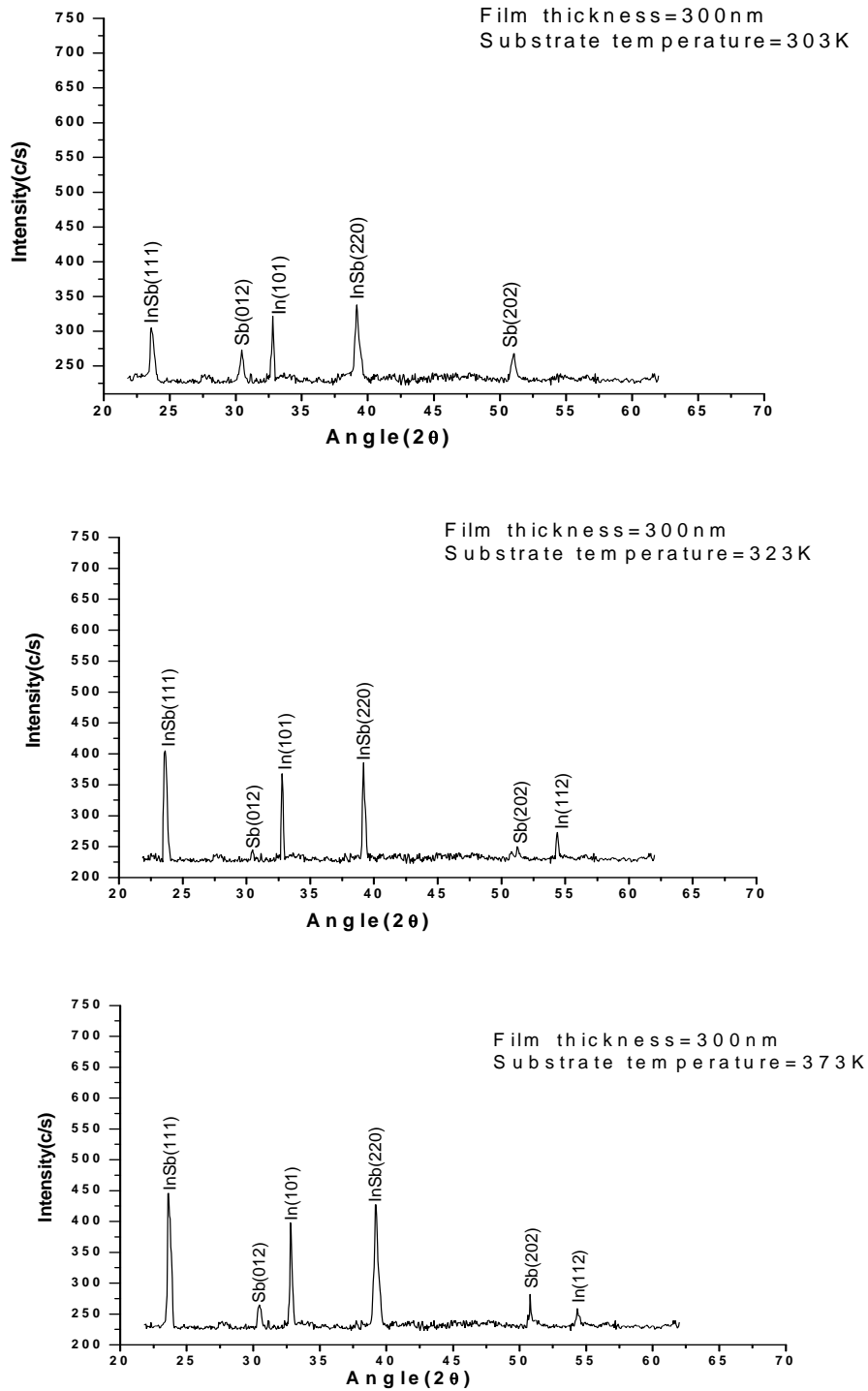


Fig.2: XRD patterns of InSb thin films of same thickness $t=300$ nm and deposited at different T_s .

We have

$$d = \left(\frac{\lambda}{2}\right) \cos ec \theta$$

So

$$\delta d = -\left(\frac{\lambda}{2}\right) (\cos ec \theta \cot \theta) \delta \theta$$

For $\theta = 90^\circ$, $\frac{\delta d}{d} = 0$.

The most accurate value of lattice parameters are estimated from the Nelson-Riley plot when $\theta = 90^\circ$. It is plotted between the calculated lattice constant values (a and c) for different planes and the error function

$$f(\theta) = \left(\frac{1}{2}\right) \left\{ \left(\frac{\cos 2\theta}{\sin \theta}\right) + \left(\frac{\cos 2\theta}{\theta}\right) \right\} \quad (7)$$

Table 1: Standard and Experimental d value of InSb.

t (nm)	Ts(K)	Diffraction angle (2θ)	(111) plane		FWHM (β)	Diffraction angle (2θ)	(220) plane		FWHM (β)
			Exp.(d) Value	Stand. (d) Value			Exp.(d) Value	Stan.(d) Value	
300	303	23.612	3.765	3.740	0.0106	39.165	2.298	2.290	0.0104
		23.613	3.763	3.740	0.0064	39.164	2.293	2.290	0.0067
		23.612	3.761	3.740	0.0058	39.162	2.292	2.290	0.0060
350	303	23.614	3.771	3.740	0.0097	39.161	2.290	2.290	0.0095
400		23.613	3.740	3.740	0.0083	39.160	2.291	2.290	0.0085

Table 2: Structural parameters of InSb thin films.

Substrate Temperature (Ts)	t (nm)	Peak intensity		Structural parameters of (111) plane			
		(111) plane	(220) plane	Grain size(D) nm	Dislocation density × 10 ¹⁵ lin/m ²	Strain × 10 ⁻³ lin ⁻² m ⁻⁴	Lattice parameter (a) × 10 ⁻¹⁰ m
303K	300	304.07	337.23	13.97	5.12	3.20	6.52
	350	339.70	350.73	15.19	4.33	3.14	6.53
	400	387.58	368.54	17.76	3.17	2.80	6.48
323K	300	404.15	386.54	23.12	1.87	2.13	6.52
373K		446.43	427.23	25.56	1.53	1.75	6.51

4. Results and Discussion

4.1 Structural analysis

The X-ray diffractographs of InSb thin films of different thicknesses and different substrate temperatures are shown in Figs.1 and 2. Films are polycrystalline having zinc blende structure. This is confirmed by comparing the observed d values of the XRD patterns of the films with the standard d values of JCPDS X-ray powder file data (#06-0208) as shown in Table 1. In these films, (111) and (220) plane is very clear and abundant.

However, a small percentage of the orientations along (012), (101), (202), and (112) planes are also observed, depending upon the film thickness and the substrate temperature of the deposition. In the case of thickness dependent InSb thin films, as thickness increases, (111) plane is dominated corresponding to (220) plane. According to substrate temperature, as substrate temperature increases, the diffracted intensity along (111) plane is also dominated by the corresponding intensity of (220) plane. The (111) plane indicates that the preferential growth of the cubic crystal in films is

along this particular direction. The (220) plane indicates that the films have hexagonal structure. The hump that is observed in the background of XRD is due to the amorphous glass substrate and also possibly due to some amorphous phase present in the InSb thin films. Different structural parameters of the InSb thin films having different thickness and grown at different Ts are calculated by using relevant formulae and systematically

given in Table 2. The data of the table show variations in the structural parameters with substrate temperature and thickness. The value of grain size (D), dislocation density (δ) and strain (ϵ) are correlated with Ts as well as with the film thickness are depicted in Figs. 3-6.

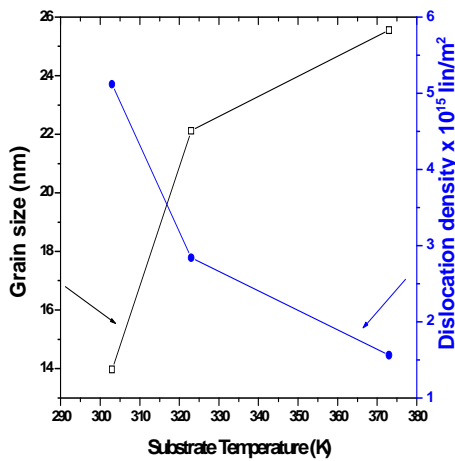


Fig.3

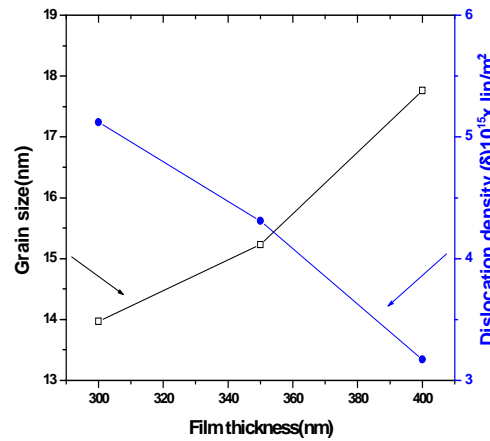


Fig.4

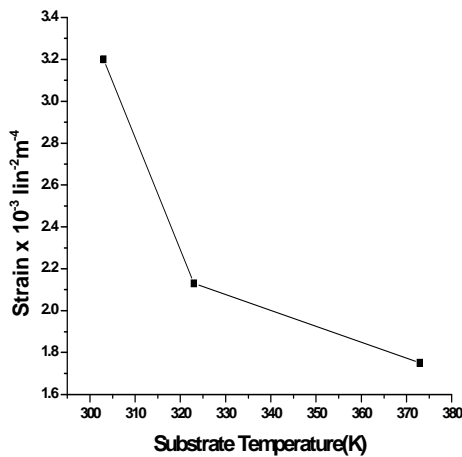


Fig.5

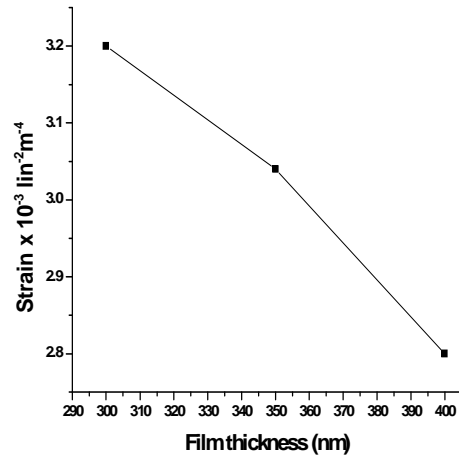


Fig.6

Figs.3-6: Variation of the grain size, dislocation density and strain with substrate temperature and thickness.

The grain sizes of the films corresponding to (111) plane has been found to increase with

substrate temperature (Ts), while dislocation density decreases. For the same plane, the grain

sizes are also found to increase and the dislocation density decreases with the thickness of thin films. With an increase in T_s , the crystallinity of the films improves substantially. In polycrystalline samples, all dislocated atoms occupy the regions which are near the grain boundaries, and from the curves it is observed that the dislocation density decreases with thickness of thin films and substrate temperature (T_s).

The decrease in dislocation density indicates the formation of high quality films as substrate temperature increases. This is possible because of fact that when the substrate temperature increases, the thermal energy of the dislocated atom increases and mobility became high.

The calculated results are in agreement with the observation on InSb thin films by earlier workers [5, 6]. At higher T_s in the formation process of the films, ad-atoms possess greater mobility along the direction parallel to substrate surface, thus contributing to the improvement of the crystallization process.

The variation of strain with the substrate temperature and thickness are shown in Figs. 5 and 6, respectively. Since the strain is a manifestation of dislocation networks, a decrease in strain indicates the formation of high quality films [11]. This may be due to a decrease in the strain energy with thickness or that the film thickness strongly affects the X-ray diffraction pattern. As thickness increases, the peaks of the films have more and more dominant effect. This work has been by Pal et al. [12].

Scanning electron micrographs (SEM) have been used for the analysis of surface morphology n-type InSb thin films. The SEM picture of n-InSb films on glass substrate are shown in Figs. 7-9. It is clearly observed that the deposited n-InSb films are nanocrystalline, homogenous, without cracks or holes, and well covered to the glass substrate. The grain size of the deposited thin films increases with an increase of the substrate temperature.

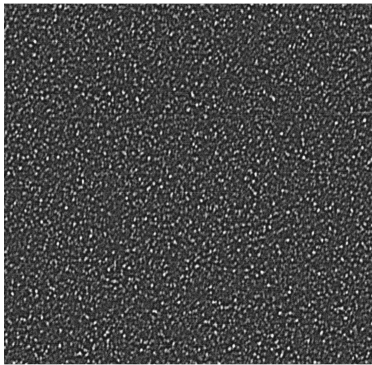


Fig.7

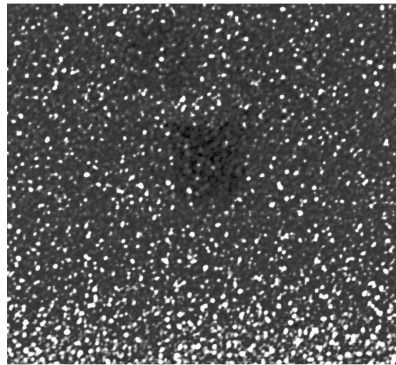


Fig.8

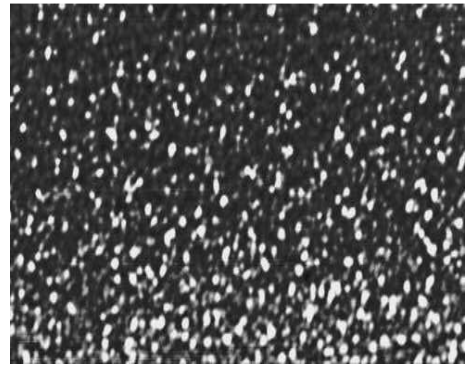


Fig.9

Figs.7-9: SEM picture of deposited thin films with different T_s (303K, 323K, 373K).

5. Conclusions

Indium antimonide thin films, deposited by the technique of electron beam evaporation within the thickness and substrate temperature range, (300-400) nm and (303-373) K, respectively, are of polycrystalline nature having zincblende structure. The films $T_s \geq 303$ are found to have an orientation along (111) and (220) planes, and only a small percentage of the growth along (012), (101), (202) & (112) are observed, depending upon the film thickness and the substrate temperature of the deposition. The crystallinity of the films improves with an increase of the substrate temperature of the

deposition. At any deposition temperature, there is a variation in grain size of the grown thin films. A decrease in the dislocation density and strain is found to be dependent on the growth temperatures and the thickness of the films. Scanning electron microscopic study confirmed the smooth surface of these films.

Acknowledgments

The authors are grateful to U.P, Council of Science & Technology, Lucknow, for providing financial support. They are highly grateful to the Head, Department of Physics, Jamia Milia Islamia

University, New Delhi, for providing XRD facility. The authors are also thankful to Professor and Head, K. Singh, Department of Physics & Electronics, Dr. R. M. L. Avadh University, Faizabadm, for providing other necessary facilities.

References

- [1] J. Heremans, D. L. Partin and C. M. Thrush, *Semicond. Sci. Technol.* **8**, 424 (1993).
- [2] M. K. Carpenter and M. W. Verbrugge, *J. Mater. Res.* **9**, 2584 (1994).
- [3] Atsushi Okamoto, Talkashi Yoshida, Shogo Muramatsu and Ichiro Shibasaki, *J. Cryst. Growth* **201**, 765 (1999).
- [4] T. Zhang, S. K. Clowes, M. Debnath, A. Bennett, C. Roberts, J. J. Harris and R. A. Stradling, *Appl. Phys. Lett.* **84**(22), (2004).
- [5] Md. Abu Taher, *Daffodil International University Journal of Science and Technology* **2**, Issue 1, 39 (2007).
- [6] V. Senithilkumar, S. Venkatachalam, C. Viswanathan, S. Gopal, D. Mangalraj, K. C. Wilson and K. P. Vijay Kumar, *Cryst. Res. Technol.* **40**(6), 573 (2005).
- [7] H. P. Klug and L. E. Alexander, *X-ray Diffraction Procedures* (John Wiley and Sons Inc., New York, 1945).
- [8] D. P. Padian, A. Marikani and K. R. Murali, *Mat. Chem. & Phys.* **78**, 51 (2002).
- [9] S. Sen, S. K. Halder and S. P. Sen, Gupta, J. *Phys. Soc. Japan* **38**, 1643 (1975).
- [10] I. H. Khan, in *Handbook of Thin Films Technology*, L.I. Maissel, R. Glang (Eds.), (McGraw-Hill Co., New York, 1970).
- [11] S. M. Sze "Physics of semiconductor devices" Second edition, May (1993).
- [12] U. Pal, D. Samanta, S. Ghorai and A. K. Chaudari, *J. Appl. Phys.* **74**, 63 (1993).
- [13] S. K. J. Al-Ani, Y. N. Obaid, S. J. Kasim, M. A. Mahdi, *Int. J. Nanoelectronics and Materials*, **2**(1), 99 (2009).

Received: 25 April, 2011

Accepted: 20 July, 2011